HHS Public Access

Author manuscript

Analyst. Author manuscript; available in PMC 2017 August 02.

Published in final edited form as:

Analyst. 2016 August 2; 141(16): 4902–4911. doi:10.1039/c6an00933f.

Expanding neurochemical investigations with multi-modal recording: simultaneous fast-scan cyclic voltammetry, iontophoresis, and patch clamp measurements

D. C. Kirkpatrick[a], **C. J. McKinney**[a], **P. B. Manis**[b,c,d], and **R. M. Wightman**[a,e]

R. M. Wightman: rmw@unc.edu

[a]Department of Chemistry, University of North Carolina at Chapel Hill, Chapel Hill, NC 27599-3290, USA

[b]Department of Otolaryngology/Head and Neck Surgery, University of North Carolina at Chapel Hill, Chapel Hill, NC, USA

[c]The Curriculum of Neurobiology, University of North Carolina, Chapel Hill, NC, USA

[d]Department of Cell Biology and Physiology, University of North Carolina, Chapel Hill, NC, USA

[e]Neuroscience Center, University of North Carolina at Chapel Hill, Chapel Hill, NC 27599-3290, USA

Abstract

Multi-modal recording describes the simultaneous collection of information across distinct domains. Compared to isolated measurements, such studies can more easily determine relationships between varieties of phenomena. This is useful for neurochemical investigations which examine cellular activity in response to changes in the local chemical environment. In this study, we demonstrate a method to perform simultaneous patch clamp measurements with fast-scan cyclic voltammetry (FSCV) using optically isolated instrumentation. A model circuit simulating concurrent measurements was used to predict the electrical interference between instruments. No significant impact was anticipated between methods, and predictions were largely confirmed experimentally. One exception was due to capacitive coupling of the FSCV potential waveform into the patch clamp amplifier. However, capacitive transients measured in whole-cell current clamp recordings were well below the level of biological signals, which allowed the activity of cells to be easily determined. Next, the activity of medium spiny neurons (MSNs) was examined in the presence of an FSCV electrode to determine how the exogenous potential impacted nearby cells. The activities of both resting and active MSNs were unaffected by the FSCV waveform. Additionally, application of an iontophoretic current, used to locally deliver drugs and other neurochemicals, did not affect neighboring cells. Finally, MSN activity was monitored during iontophoretic delivery of glutamate, an excitatory neurotransmitter. Membrane depolarization and cell firing were observed concurrently with chemical changes around the cell resulting from delivery. In all, we show how combined electrophysiological and electrochemical measurements can relate information between domains and increase the power of neurochemical investigations.

Correspondence to: R. M. Wightman, rmw@unc.edu.

Introduction

Neurochemical systems are analyzed by a variety of methods, which can characterize distinct events such as cell firing, neurotransmitter release, and changes in blood flow.[1,2] Information collected simultaneously from multiple domains, termed multi-modal recording, helps to reveal relationships between variables that may be otherwise too difficult to surmise from isolated or independent measurements. This is beneficial for studies that need to link events between domains, such as the relationship between cellular activity and exocytosis, the influence of neurotransmitters on vascular coupling, or the behaviors of interconnected cells.[3–10] Two popular domains which have recently undergone rapid growth in neurochemical studies are the electrophysiological, which provides information about cellular activity, and the electrochemical, used to study the local chemical environment. These can be combined using distinct sensors, or both executed at a single electrode.[11]

The whole-cell patch clamp is a commonly employed electrophysiological method that uses a micropipette to manipulate and record cell behavior.[12] It has two modes of operation: voltage clamp, typically used to study ion channels, and current clamp, which records the cell membrane potential. Patch clamp electrophysiology has been successfully incorporated in multi-modal investigations with amperometry, which provides information in the chemical domain.[13–15] Although simple to incorporate, amperometry limits information about the chemical environment since it only allows for the detection of a singular analyte, and does not provide information about the identity of the detected chemical. In comparison, fast-scan cyclic voltammetry (FSCV), which utilizes a triangular potential waveform scanned rapidly across a carbon-fiber microelectrode, can differentiate between multiple electroactive species and offers qualitative information regarding their identities.[16] In addition, carbon-fiber electrodes can be used to detect a broad range of neurochemical events, such as changes in pH, single unit activity, and even ionic changes.[11,17] Incorporation of FSCV with patch clamp electrophysiology would improve the ability of neurochemical investigations to obtain and relate information spread over multiple domains.

In this work we demonstrate a method to combine patch clamp and FSCV instrumentation. Since both techniques require precise current and voltage measurements, a model circuit is first developed to determine the anticipated electrical crosstalk between instruments. Upon analysis both methods were predicted to operate without interference, and the experimental results largely confirmed this. Once validated, whole-cell current clamp measurements were performed to monitor cellular activity in the presence of exogenously applied FSCV potential. Although currents generated during FSCV could theoretically excite or damage cells if coupled into the membrane, no change in cell behavior was observed. Additionally, currents administered during iontophoresis, a drug delivery method which uses an electric current to eject a solution from a glass capillary, were also determined not to impact nearby cells. Lastly, application of combined measurements is demonstrated by monitoring cell behavior during iontophoresis of glutamate, an excitatory neurotransmitter. In all, we exhibit the feasibility and utility of multi-modal patch and FSCV measurements.

Experimental

Chemicals and solutions

All chemicals were used as received from Sigma Aldrich (St Louis, MO). Recording artificial cerebral spinal fluid (aCSF) consisted of 126 mM NaCl, 2.5 mM KCl, 1 mM NaH_2PO_4, 26 mM $NaHCO_3$, 2 mM $MgSO_4$, 2 mM $CaCl_2$, and 11 mM glucose. After oxygenation (95% O_2, 5% CO_2) the pH was adjusted to 7.4. Iontophoretic solutions were made daily from filtered (0.45 μm Nylon, Nalgene, USA) DI water. Their pH measured between 6 and 7.

Animal care and use

Male Sprague-Dawley rats (250–300 g, Charles River, Wilmington, MA) were used for all experiments. Rats were dually housed on a 12/12 hour day/night cycle and provided with food and water *ad libitum*. Special care was given to minimize the number of animals and to reduce their suffering. All procedures were approved by the Institutional Animal Care and Use Committee at the University of North Carolina at Chapel Hill.

Brain slice preparation

Following anesthesia with urethane (1.5 g kg^{-1}), brains were quickly removed and submerged into oxygenated (95% O_2, 5% CO_2) chilled sucrose-based aCSF (185 mM sucrose, 2.5 mM KCl, 1.2 mM KH_2PO_4, 25 mM $NaHCO_3$, 25 mM glucose, 10 mM $MgSO_4$, and 0.5 mM $CaCl_2$, adjusted to pH = 7.4). A vibratome (VF-200, Precisionary Instruments, San Jose, CA) fitted with a stainless steel blade (Fendrihan, USA) was used to obtain 300 μm thick coronal slices containing the nucleus accumbens (NAc). After cutting, these were immediately transferred to room temperature (20 °C) recording aCSF and allowed 1 hour to recover. During experiments, slices were anchored (SHD-22KIT, Warner Instruments, Hamden, CT) in a perfusion chamber (RC-22, Warner Instruments) on the stage of an Eclipse FN1 microscope (Nikon Instruments, Melville, NY), which sat atop a vibration free table (TMC, Peabody, MA). A 30 min period of continuous perfusion (2 mL min^{-1}) with 37 °C recording aCSF was given prior to analysis.

Patch clamp electrophysiology

Patch pipettes were fabricated from borosilicate capillaries (1.5/0.86 mm O.D./I.D., Sutter Instruments) using a PC-84 micropipette puller (Sutter Instruments). Pipettes were filled with an intracellular solution consisting of 126 mM K-gluconate, 6 mM KCl, 2 mM NaCl, 10 mM HEPES, 1 mM EGTA, 10 mM phosphocreatine, 4 mM Mg-ATP, and 0.3 mM Na_2-GTP which was adjusted to pH = 7.2 and measured between 260 and 290 mOsm. An Ag wire coated with AgCl was used to connect the pipette to the headstage. The pipette resistance was determined using a 0–10 mV potential step, and consistently measured between 6 and 9 MΩ. Visualization of cells in the NAc core was achieved using asymmetric illumination.[18] Images were obtained through a 40× immersion objective (Nikon Instruments), captured on a CMOS camera (Rolera Bolt, QImaging, Surrey, BC), and displayed with associated software (Q-Capture Pro 7, QImaging). Medium spiny neurons (MSNs) were distinguished from interneurons based on size. Once identified, a

micromanipulator (MP-285 with MPC-200- ROE and controller, Sutter Instruments, Novato, CA) was used to position the patch pipette near the cell. Following formation of a GΩ seal, a whole-cell patch was obtained by applying suction to the pipette. Recordings were made with an Axopatch 200B patch clamp amplifier (Axon Instruments, Foster City, CA). Cell parameters were determined from a 10 mV step applied from a −75 mV potential. Membrane resistance (69 ± 4 MΩ, SEM, $n = 39$) and capacitance (78 ± 3 pF, SEM, $n = 39$) were used in conjunction with the response to intracellular current steps to confirm correct identification of cells.[19–22] Only trials where the pipette access resistance measured below 35 MΩ and changed less than 25% during experiments were included. A Ag/AgCl electrode (World Precision Instruments, Sarasota, FL) was used as a reference, and also served as the iontophoresis current return electrode. Whole-cell currents and voltages were low-pass filtered at 2 kHz, digitized at 10 kHz (Digidata 1320A Axon Instruments), and recorded using Clampex 10.3 software (Molecular Devices, Silicon Valley, CA). Pipette offset potential and pipette capacitance compensation controls were adjusted prior to forming a GΩ seal. Whole cell capacitance and series resistance were 75% compensated in voltage clamp. For current clamp measurements, series resistance was fully compensated.

Fast-scan cyclic voltammetry

Multibarreled iontophoresis probes containing a T-650 carbon-fiber electrode were constructed from pre-fused borosilicate capillaries (Friedrich & Dimmock, Millville, NJ) as previously described.[23] The carbon fiber was cut to 100 μm and served as the FSCV electrode. Connection to the headstage was made with a stainless steel wire inserted into the electrode barrel, which contained a 4 M CH_3COOK and 0.15 mM NaCl solution. A micromanipulator (MPC-200-ROE, Sutter Instruments) was used to position the probe near visually identified cells. Measurements were obtained using a triangular waveform and applied from a homemade instrument (UEI, UNC Chemistry Electronics Facility, UNC Chapel Hill). Unless otherwise stated, the waveform consisted of a −0.4 V holding potential with an upper limit of 1.0 V, scanned at 600 V s^{-1}, and repeated at 5 Hz. For detection of DOPAC, the holding potential was lowered to −0.8 V. Waveform parameters and data collection were accomplished with HDCV software through a PCIe-6363 DAQ card (National Instruments).[24] Prior to analysis, data underwent filtering (2–16 kHz), background subtraction, and signal averaging.

Initial simultaneous FSCV and patch clamp measurements yielded significant 60 Hz noise. To address this, different Ag/AgCl reference electrodes were used for each instrument.[25] Signals were further isolated by connecting the FSCV return electrode to a negative battery terminal, while the patch reference electrode remained at AC power ground. This required battery operation of the UEI, which generated the FSCV waveform applied at the electrode (Fig. 1A). Additionally, since all commands originated at the AC ground-referenced CPU of a personal computer, an optical isolator (UNC Chemistry Electronics Facility) was used to transduce FSCV command signals to the battery-referenced potential prior to reaching the UEI (Fig. 1B). Current generated at the carbon-fiber electrode underwent the reverse process prior to recording. The FSCV current was measured by the UEI, transduced to AC power ground, and recorded at the CPU.

Iontophoresis

The remaining barrels on the multibarreled carbon-fiber probes were used for iontophoretic ejections. After pulling, drug barrels had diameters of 0.5 to 1.0 μm. Ejection currents were administered from a locally constructed instrument (UNC Chemistry Electronics Facility), which was controlled using customized LabVIEW software (National Instruments, Austin, TX) and an NI-USB 6343 DAQ card (National Instruments). A Ag/AgCl electrode (World Precision Instruments, Sarasota, FL) held at AC power ground was used as the counter electrode.

Results and discussion

Modeling the collective use of patch clamp, FSCV, and Iontophoresis instrumentation

A model circuit was developed which simulated concurrent FSCV and patch clamp measurements. This is depicted in Fig. 2, in which a cell is patched in whole-cell mode with the corresponding circuit components detailed in Table 1. Here, we focus specifically on the current clamp method for patch measurements. In this configuration, the cell membrane voltage is recorded by the patch amplifier, which is also used to administer intracellular current injections. Chemical changes around the cell are detected by the FSCV current on a carbon-fiber microelectrode, which is controlled by the universal electrochemical instrument (UEI). Also included is iontophoresis, a drug delivery method which uses an electrical current applied from a constant source to eject solution from a micropipette. To determine if FSCV and patch measurements would be obscured by the incorporation of other methods, the amount of crosstalk, or electrical interference between instruments, was calculated. For example, in FSCV the maximum potential applied to the electrode rarely exceeds 1.4 V.[26,27] From this voltage, the model predicts measurements of the membrane potential performed by the patch amplifier will be overestimated by 0.035 mV. Similarly a 1 μA iontophoretic ejection, the maximum current deliverable by many commercially available iontophoretic instruments, was calculated to increase measurements by 0.075 mV.[28–30] Since both of these values are below the 1 mV noise level common to most current clamp instruments, FSCV and iontophoresis were not expected to significantly impact recordings made of the membrane potential. For FSCV measurements, a 1 μA iontophoresis ejection was calculated to add 0.025 nA to the current at the carbon-fiber electrode. Similarly a 500 pA intracellular injection delivered by the patch amplifier was predicted to increase the FSCV current by 0.5 pA. Both of these values are below the noise in FSCV recordings, which rarely exceeds 0.3 nA.[31,32] Thus no significant electrical coupling or crosstalk was anticipated between instruments.

FSCV signal unaffected by patch and iontophoretic currents

To experimentally determine the effect of patch and iontophoretic currents on FSCV measurements, a carbon-fiber microelectrode contained in a multibarreled probe was inserted into the nucleus accumbens (NAc) core of a rat brain slice. The three other barrels on the probe contained an NaCl solution for iontophoresis ejections. A patch pipette was positioned roughly 10 μm from the carbon fiber. For simplicity, the patch pipette in initial experiments was not attached to a cell, but was still operated in current clamp mode. First, the FSCV signal was examined by measuring elicited dopamine (DA) release, which was

electrically evoked using a bipolar stimulating electrode. During this time, both the patch pipette and iontophoretic barrels maintained zero net current. Fig. 3A displays a color plot showing the background subtracted FSCV current following evoked release (middle). A vertical cross-section (dashed blue line) taken just after stimulation reveals the cyclic voltammogram of DA (upper), which confirms the identity of the chemical signal. Similarly a horizontal cross-section along the DA oxidation potential (dashed white line) reveals the DA oxidation current *versus* time (lower), and shows the time-course of release. Inspection of the current in the absence of DA revealed ~0.1 nA of noise from the baseline, which compares favorably to FSCV measurements performed in isolation.

Next, current was delivered from the patch pipette to study its effect on the FSCV signal. Fig. 3B displays the FSCV current along the DA oxidation potential during successive current steps. No effect was observed on the FSCV signal. This occurred despite no cell attached to the patch pipette, which should have amplified crosstalk between instruments. Thus as predicted from the model circuit, current administered from the patch pipette did not affect FSCV measurements. Subsequently, the effect of the iontophoresis ejection current on FSCV measurements was examined by ejecting NaCl solutions from the iontophoretic barrels. Fig. 3C displays the current along the DA oxidation potential as iontophoretic current was applied step-wise between 0.5 and 1.5 μA. Rapid deflections were observed when the ejection current was changed to a new value. Since these deflections quickly returned to the baseline, they were attributed to capacitive coupling between the iontophoresis barrel and the carbon fiber. If caused by direct current flow between the iontophoresis barrel and carbon fiber, the signal would have shown a baseline shift sustained throughout the ejection. However this did not occur, as the FSCV current was unaffected shortly after the deflections subsided. Together, these experiments confirmed calculations from the model predicting neither patch nor iontophoretic current would interfere with FSCV measurements.

Effect of FSCV waveform on patch recordings

Next, the ability to perform patch clamp recordings during FSCV was examined. To accomplish this, a medium spiny neuron (MSN) in the NAc core of a brain slice was patched in whole-cell mode. A multibarreled iontophoresis probe containing a carbon-fiber electrode was positioned approximately 10 μm from the cell body. For FSCV, a triangular waveform was applied to the carbon-fiber electrode between −0.4 to +1.0 V at 600 V s^{-1}, repeating at 5 Hz. Due to the lack of excitatory glutamatergic tone in the slice, MSNs resided in a down, or resting state, and required a depolarizing stimulus to initiate firing.[33,34] Fig. 4A shows a current clamp recording of the MSN membrane potential during FSCV at an adjacent carbon-fiber electrode, which shows repetitive transients centered on the resting potential. These transients occurred at an identical frequency to the FSCV waveform, and disappeared when the waveform was disabled. Additionally, their magnitude, which ranged between 2–4 mV from the baseline, was unaffected by the distance between the carbon fiber and patch pipette. When further examined, transients had a similar appearance to the unsubtracted FSCV current at the carbon-fiber electrode (Fig. 4B and C). Whole-cell voltage clamp measurements also contained transients, but these appeared as the inverse of the FSCV current (Fig. 4D).

To determine the cause of transients, parameters of the FSCV waveform were varied while the effect on the current clamp signal was observed. First, the limits of the triangular waveform were lowered from −0.4 and +1.0 V to −0.7 and +0.7 V, while a consistent scan rate (600 V s^{-1}) was maintained. This had no effect on the transient magnitude, indicating they were not caused by direct current between the carbon fiber and patch pipette. Next, the scan rate of the waveform was varied while maintaining constant voltage limits. As shown in Fig. 4E, the transient magnitude increased with the scan rate. These results indicated that transients were due to capacitive coupling of the FSCV waveform into the patch recordings. This is because capacitive current (i_c) is generated in proportion to the rate of change of a voltage, $i_c = C(\mathrm{d}V/\mathrm{d}t)$, and is independent of the magnitude of the potential. Since capacitive rather than direct current was the source of transients, recordings made when the FSCV potential was constant were not affected. This occurs between triangular ramps, when a holding potential is applied to promote analyte adsorption to the electrode surface.[27,35] During this period, measurements of the membrane potential were identical to those made with the waveform disabled.

Cell firing and shifts in the membrane potential can still be reliably monitored in the presence of an FSCV electrode because the holding potential accounts for a majority of the total voltammetric period. For example, during the 5 Hz waveform utilized in Fig. 4A, the triangular portion was applied just 2.3% of the time. However if recordings without capacitive transients are desired, there are several methods to minimize or remove them while still collecting electrochemical information. First, since capacitive coupling is proportional to $\mathrm{d}V/\mathrm{d}t$, a lower FSCV scan rate will reduce the size of transients (Fig. 4E). Indeed at sufficiently low scan rates (<200 V s^{-1}), transients could be eliminated entirely. However this may not be desirable in certain cases because it is accompanied by a decrease in the FSCV electrode sensitivity.[36] Alternatively, some patch amplifiers are equipped with cross capacitance neutralization circuits, which may be used to eliminate transients from recordings without altering the FSCV waveform parameters.

Effect of iontophoretic current on patch recordings

We then investigated whether current clamp measurements were affected by iontophoretic current. To do this, the patch pipette voltage was monitored during iontophoretic ejections of NaCl. Experiments were performed in the absence of a cell to ensure that changes in the measured pipette potential were due to the iontophoretic current rather than cellular activity. Fig. 4F reveals that the pipette potential increased proportionally with the iontophoretic current. Because the voltage offset was sustained throughout the ejection period, the change in potential could be attributed to direct current flow between the iontophoretic and patch pipettes. Measurements of the average error, 0.89 mV per μA of iontophoretic current (n = 5), were similar to those made when a cell was attached, and were roughly an order of magnitude greater than the model predicted. Most likely this was due to polarization at the iontophoretic barrel tip during ejections, which altered the current flow predicted in the model.[37,38] Nevertheless the observed offset was small compared to anticipated signals. In fact, since most iontophoretic ejections employ currents from the 10's to 100's of nA, errors incurred during ejections would still likely be contained within the noise.[39] Thus in practice,

iontophoretic current was determined not to have a significant impact on current clamp measurements.

Cell response to exogenous potential and current

After establishing the ability to accurately perform current clamp measurements concurrently with FSCV and iontophoresis, we next examined how these techniques affected nearby cells. Since the behavior of many neuronal components is voltage dependent, cells neighboring the carbon-fiber probe may be affected by exogenous potential and current inherent to these methods. To study this, a carbon fiber contained in a multibarreled iontophoresis probe was positioned ~10 μm from the soma of an MSN. A whole-cell patch was performed and the membrane potential of the resting cell was examined while the FSCV waveform was alternated on and off. Fig. 5A demonstrates that besides capacitive transients, no difference was observed between periods when the waveform was applied (red bars) and disabled. The cell maintained its resting potential and no firing was initiated. Next, the effect of the FSCV waveform on excited cells was examined. Using current steps administered from the patch pipette, cells were progressively depolarized until firing was achieved (Fig. 5B). Consistent with well-established behavior, MSNs displayed strong inward rectification, a voltage ramp preceding firing, and a delayed initial action potential.[40] Additionally both the rheobase, the current required to induce firing, and the threshold potential, the membrane voltage which must be reached to initiate firing, were unaffected by the FSCV waveform (paired t test, $P = 0.753$, $P = 0.744$ respectively, $n = 13$). Thus no difference was observed in the resting or active state of cells due to exogenous FSCV potential.

Next, the effect of iontophoretic ejections on cell behavior was examined. Since iontophoretic currents are several orders of magnitude greater than the rheobase, it has been suggested that ejection currents may perturb nearby cells.[41] In fact, some commercial iontophoretic systems attempt to offset the ejection current with an equal and opposite balancing current applied through a separate barrel. To study how the iontophoretic current affected cells, MSN firing was observed during ejection of NaCl. First, a depolarizing current injection was applied from the patch pipette to transition cells into an active state, where firing occurred at a constant frequency (Fig. 6). Next, an iontophoretic barrel located next to the cell delivered the ejection current. If the iontophoretic current impacted cells, the firing rate would have increased due to the additional excitatory stimulus. However, no change in the firing frequency was observed for ejection currents up to 40 μA, even without the use of balancing currents. The only effect was a slight offset in the voltage measured by the patch pipette, most visible during the 800 nA ejection, which as shown by Fig. 4F occurs independently of cellular activity. This is significant because currents used for iontophoretic ejections are much greater than the rheobase of cells. However, no increase in the firing rate was observed, indicating that the ejection current was carried by the highly conductive extracellular solution rather coupling into the cell.

Applications of combined instrumentation

To demonstrate simultaneous patch and FSCV measurements, glutamate, an excitatory neurotransmitter, was iontophoretically applied to MSNs while cellular activity was recorded. Ejections were monitored by FSCV using a method termed controlled

iontophoresis, in which the ejection of an electro-active analyte is detected by the carbon fiber.[42,43] Since glutamate is not electroactive, the iontophoretic solution also contained 3,4-dihydroxyphenylacetic acid (DOPAC). DOPAC had no effect on MSNs, but its oxidation on the carbon fiber served as an electrochemical marker for ejections.[44] This allowed the time-course of glutamate delivery and the relative ejection quantity to be determined.

Fig. 7A displays the membrane potential of an MSN (black) during iontophoretic delivery (red bars). As the iontophoretic current was increased, the cell became increasingly depolarized and firing was initiated. This was due to a greater ejection concentration of glutamate, represented by the DOPAC oxidation current (7A, blue) and FSCV color plot in 7B. The time-course of the −30 nA ejection is shown in Fig. 7C. Detection of the ejection marker occurred almost immediately after the iontophoretic current was initiated. Due to the time required for glutamate to reach the cell and act upon receptors, membrane depolarization was slightly delayed.[45] Cell firing occurred as the marker current peaked, and quickly ceased once it approached the pre-ejection quantity.

Conclusions

We have demonstrated how simultaneous patch clamp and FSCV measurements can be successfully incorporated into multi-modal investigations. Their combined use allows cell behavior to be examined concurrently with changes in the chemical, metabolic, and ionic environment. It was also determined that cells are not affected by exogenous electrical potentials and currents inherent to FSCV and iontophoresis. Collective use of these methods increases the power of neurochemical studies to correlate information across multiple domains.

Acknowledgments

Electrochemical and iontophoretic instruments were constructed by the University Of North Carolina Department Of Chemistry Electronics Facility. Additional assistance was provided by Mathew Verber. The contributions of Luke Campagnola in assembling patch clamp instrumentation and development of related protocols are greatly appreciated. Funding was provided by the NIH (DA010900 to RMW and DC009809 to PBM).

References

1. Michael, AC.; Borland, LM., editors. Electrochemical Methods for Neuroscience. Boca Raton, FL: CRC Press; 2007.
2. Vertes, RP.; Stackman, RW., Jr, editors. Electrophysiological Recording Techniques. 1st. New York City, NY: Humana Press; 2011.
3. Galarreta M, Hestrin S. Nature. 1999; 402:72–75. [PubMed: 10573418]
4. Yamamoto K, Koyanagi Y, Koshikawa N, Kobayashi M. J. Neurophysiol. 2010; 104:1933–1945. [PubMed: 20685921]
5. Sheth SA, Nemoto M, Guiou M, Walker M, Pouratian N, Toga AW. Neuron. 2004; 42:347–355. [PubMed: 15091348]
6. Oberhauser AF, Robinson IM, Fernandez JM. Biophys. J. 1996; 71:1131–1139. [PubMed: 8842250]
7. Phongphanphanee P, Kaneda K, Isa T. J. Neurosci. 2008; 28:9309–9318. [PubMed: 18784311]
8. Henze DA, Borhegyi Z, Csicsvari J, Mamiya A, Harris KD, Buzsáki G. J. Neurophysiol. 2000; 84:390–400. [PubMed: 10899213]
9. Lu H, Hartmann MJ, Bower JM. J. Neurophysiol. 2005; 94:1849–1860. [PubMed: 15928051]

10. Cepeda C, Galvan L, Holley SM, Rao SP, André VM, Botelho EP, Chen JY, Watson JB, Deisseroth K, Levine MS. J. Neurosci. 2013; 33:7393–7406. [PubMed: 23616545]
11. Takmakov P, McKinney CJ, Carelli RM, Wightman RM. Rev. Sci. Instrum. 2011; 82:074302. [PubMed: 21806203]
12. Sakmann B, Neher E. Sci. Am. 1992; 266:44–51. [PubMed: 1374932]
13. Galli A, Blakely RD, DeFelice LJ. Proc. Natl. Acad. Sci. U. S. A. 1998; 95:13260–13265. [PubMed: 9789076]
14. Oberhauser AF, Fernandez JM. Proc. Natl. Acad. Sci. U. S. A. 1996; 93:14349–14354. [PubMed: 8962054]
15. Moser T, Chow RH, Neher E. Pflügers Arch. 1995; 431:196–203. [PubMed: 9026779]
16. Bucher ES, Wightman RM. Annu. Rev. Anal. Chem. 2015; 8:239–261.
17. Takmakov P, Zachek MK, Keithley RB, Bucher ES, McCarty GS, Wightman RM. Anal. Chem. 2010; 82:9892–9900. [PubMed: 21047096]
18. Kachar B. Science. 1985; 227:766–768. [PubMed: 3969565]
19. Lepora NF, Blomeley CP, Hoyland D, Bracci E, Overton PG, Gurney K. Eur. J. Neurosci. 2011; 34:1390–1405. [PubMed: 22034974]
20. Gustafson N, Gireesh-Dharmaraj E, Czubayko U, Blackwell KT, Plenz D. J. Neurophysiol. 2006; 95:737–752. [PubMed: 16236782]
21. Kawaguchi Y. J. Neurosci. 1993; 13:4908–4923. [PubMed: 7693897]
22. Ibáñez-Sandoval O, Tecuapetla F, Unal B, Shah F, Koós T, Tepper JM. J. Neurosci. 2010; 30:6999–7016. [PubMed: 20484642]
23. Belle AM, Owesson-White C, Herr NR, Carelli RM, Wightman RM. ACS Chem. Neurosci. 2013; 4:761–771. [PubMed: 23480099]
24. Bucher ES, Brooks K, Verber MD, Keithley RB, Owesson-White C, Carroll S, Takmakov P, McKinney CJ, Wightman RM. Anal. Chem. 2013; 85:10344–10353. [PubMed: 24083898]
25. Ott, H. Noise Reduction Techniques in Electrochemical Systems. 2nd. New York, NY: John Wiley & Sons, Inc.; 1988.
26. Hafizi S, Kruk ZL, Stamford JA. J. Neurosci. Methods. 1990; 33:41–49. [PubMed: 2232859]
27. Heien MLAV, Phillips PEM, Stuber GD, Seipel AT, Wightman RM. Analyst. 2003; 128:1413–1419. [PubMed: 14737224]
28. 6400 Advanced Micro-Iontophoresis Current Generator Operating Manual. Minneapolis, MN: Dagan Corporation; 2008.
29. WPI Model 260 Instruction Manual. Sarasota, FL: World Precision Instruments; 2000.
30. Neurophore BH-2 Micro-Iontophoresis System User's Manual. Hamden, CT: Harvard Apparatus; 2016.
31. Keithley RB, Mark Wightman R, Heien ML. TrAC, Trends Anal. Chem. 2009; 28:1127–1136.
32. Johnson JA, Rodeberg NT, Wightman RM. ACS Chem. Neurosci. 2016; 7:349–359. [PubMed: 26758246]
33. Azdad K, Gall D, Woods AS, Ledent C, Ferre S, Schiffmann SN. Neuropsychopharmacology. 2008; 34:972–986. [PubMed: 18800071]
34. Vergara R, Rick C, Hernandez-Lopez S, Laville JA, Guzman JN, Galarraga E, Surmeier DJ, Bargas J. J. Physiol. 2003; 553:169–182. [PubMed: 12963790]
35. Swamy BEK, Venton BJ. Anal. Chem. 2007; 79:744–750. [PubMed: 17222045]
36. Keithley RB, Takmakov P, Bucher ES, Belle AM, Owesson-White CA, Park J, Wightman RM. Anal. Chem. 2011; 83:3563–3571. [PubMed: 21473572]
37. Shi W, Sa N, Thakar R, Baker LA. Analyst. 2015; 140:4835–4842. [PubMed: 25118339]
38. Yusko EC, An R, Mayer M. ACS Nano. 2010; 4:477–487. [PubMed: 20028119]
39. Herr NR, Wightman RM. Front. Biosci., Elite Ed. 2013; 5:249–257. [PubMed: 23276986]
40. Planert H, Szydlowski SN, Hjorth JJJ, Grillner S, Silberberg G. J. Neurosci. 2010; 30:3499–3507. [PubMed: 20203210]
41. Bloom FE. Life Sci. 1974; 14:1819–1834. [PubMed: 4368008]
42. Armstrong-James M, Millar J. Nature. 1980; 288:181–183. [PubMed: 7432519]

43. Herr NR, Kile BM, Carelli RM, Wightman RM. Anal. Chem. 2008; 80:8635–8641. [PubMed: 18947198]
44. Kirkpatrick DC, Walton LR, Edwards MA, Wightman RM. Analyst. 2016; 141:1930–1938. [PubMed: 26890395]
45. Kirkpatrick DC, Edwards MA, Flowers PA, Wightman RM. Anal. Chem. 2014; 86:9909–9916. [PubMed: 25157675]

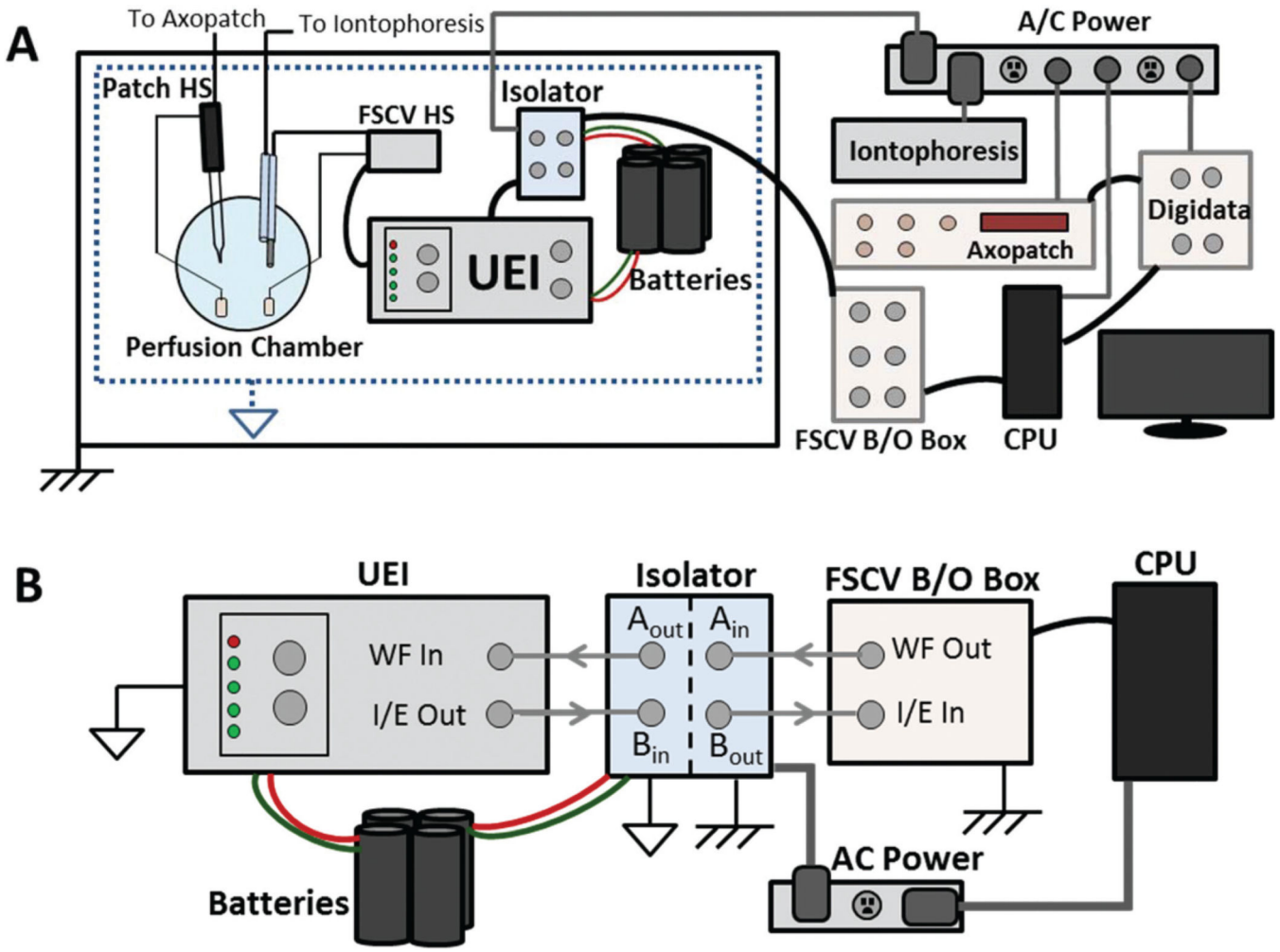

Fig. 1.

Instrumentation for combined recordings. (A) Block diagram of FSCV, patch clamp, and iontophoresis instruments. Patch clamp commands are generated at the CPU, amplified (Digidata, Axopatch), and applied at the patch headstage. All components are referenced to AC ground. Similarly, iontophoresis currents are AC ground-referenced. For FSCV, commands originate at the CPU referenced to AC ground. These are amplified (B/O box) and transduced (isolator) to a battery-referenced potential. The UEI, powered by the battery, receives the command and applies the waveform at the electrode. (B) Transduction of FSCV signals. The waveform command is sent from the CPU to the isolator ('WF Out' to 'A_{in}'), and arrives at the UEI after transduction ('A_{out}' to 'WF in'). FSCV current is transduced through the isolator ('*I/E* out' to 'B_{in}') and recorded by the CPU ('B_{out}' to '*I/E* in').

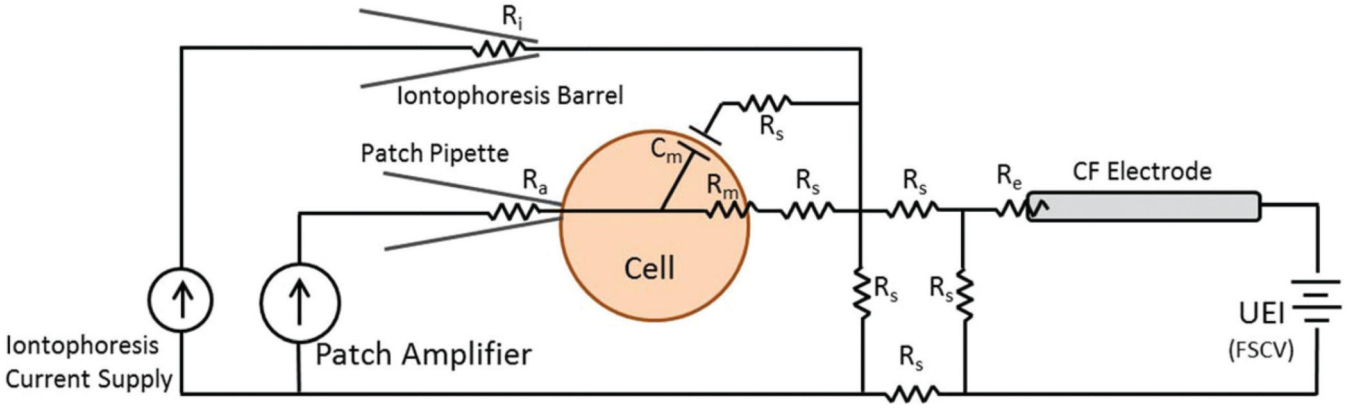

Fig. 2.

Model circuit for combined operation of FSCV, patch clamp, and iontophoresis instruments. The patch pipette is controlled by the patch amplifier, operating in whole-cell mode. FSCV is performed on the carbon-fiber electrode, which is connected to a potentiostat (UEI). Iontophoretic ejections are administered by a constant current source.

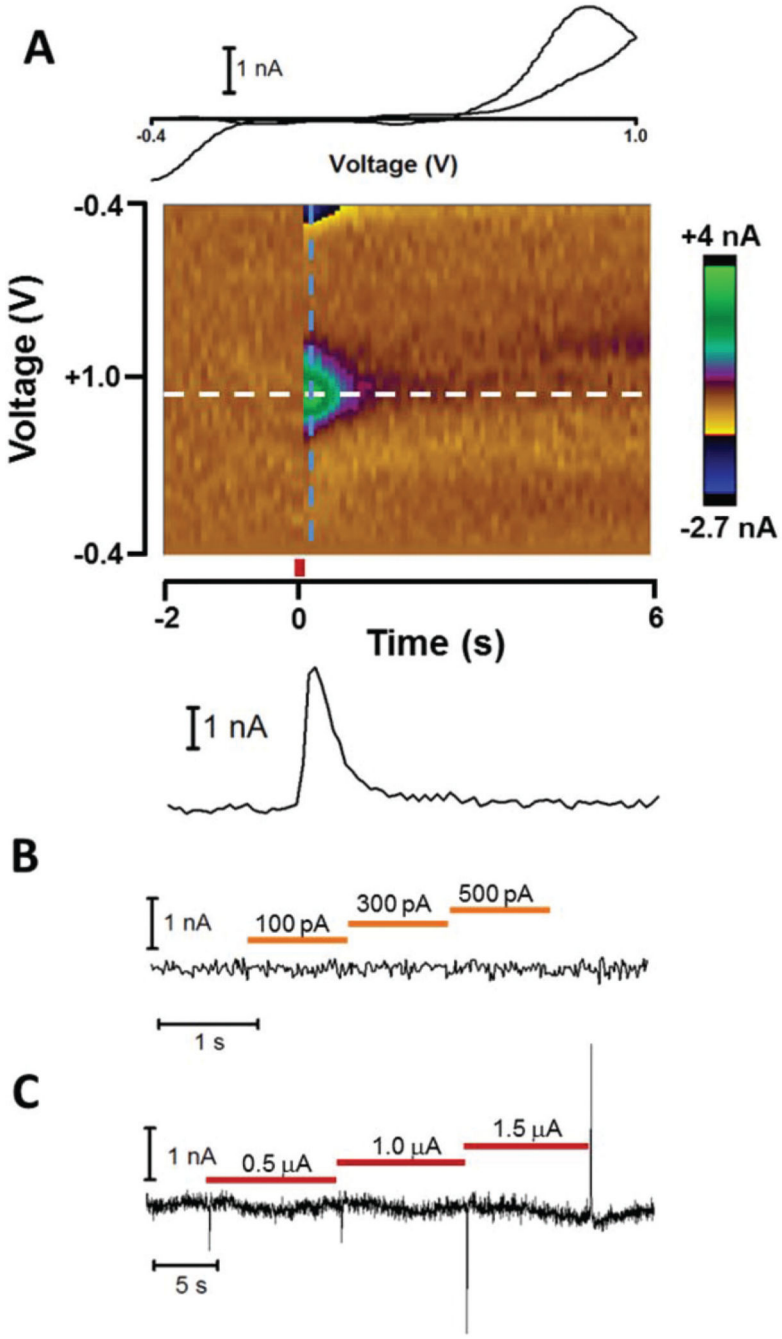

Fig. 3.

Effect of patch and iontophoresis instruments on FSCV measurements. (A) FSCV response to electrically evoked DA release. A carbon-fiber electrode detected electrically evoked DA release in the NAc core of a rat brain slice while a neighboring patch pipette and iontophoresis barrel maintained zero net current. The DA CV (upper) was obtained from the color plot (middle) using the current across the waveform just after stimulation (dashed blue line). A DA current *versus* time trace (lower) was generated from the current at the DA oxidation potential over the time-course of the measurement. Stimulation (red bar) occurred

at $t = 0$. (B) FSCV signal along the DA oxidation potential during current steps administered by the patch pipette. Orange bars represent the time of the applied current. (C) FSCV signal along the DA oxidation potential during iontophoretic ejection (red bars) of NaCl.

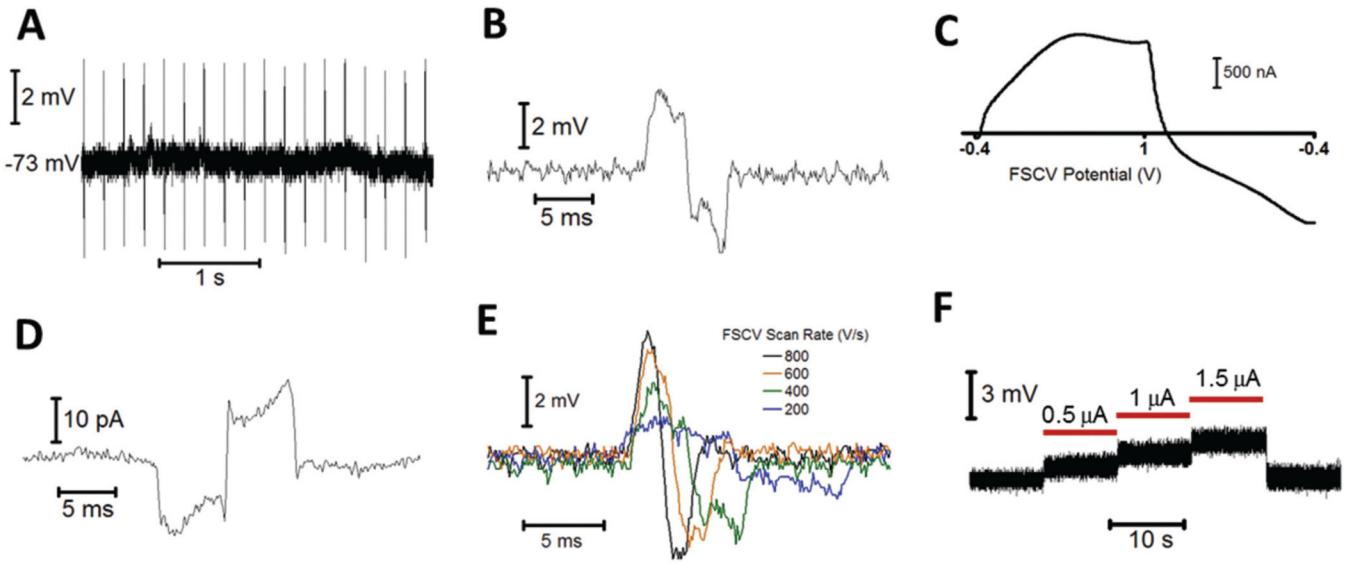

Fig. 4.

Effect of FSCV and iontophoresis instruments on patch clamp measurements. (A) Whole-cell current clamp recording of the spontaneous membrane potential of an MSN in the presence of a carbon-fiber electrode performing FSCV. (B) A magnified transient from A. (C) The unsubtracted FSCV current at the carbon-fiber electrode from A. (D) Whole-cell voltage clamp recording (v_m = −75 mV) of an MSN, made in the presence of a carbon fiber performing FSCV. (E) Transients recorded in a whole-cell current clamp for different scan rates at the FSCV electrode. The waveform maintained constant limits between −0.4 and 1.0 V. (F) Current clamp recording of the patch pipette voltage during iontophoretic ejections (red bars) of NaCl.

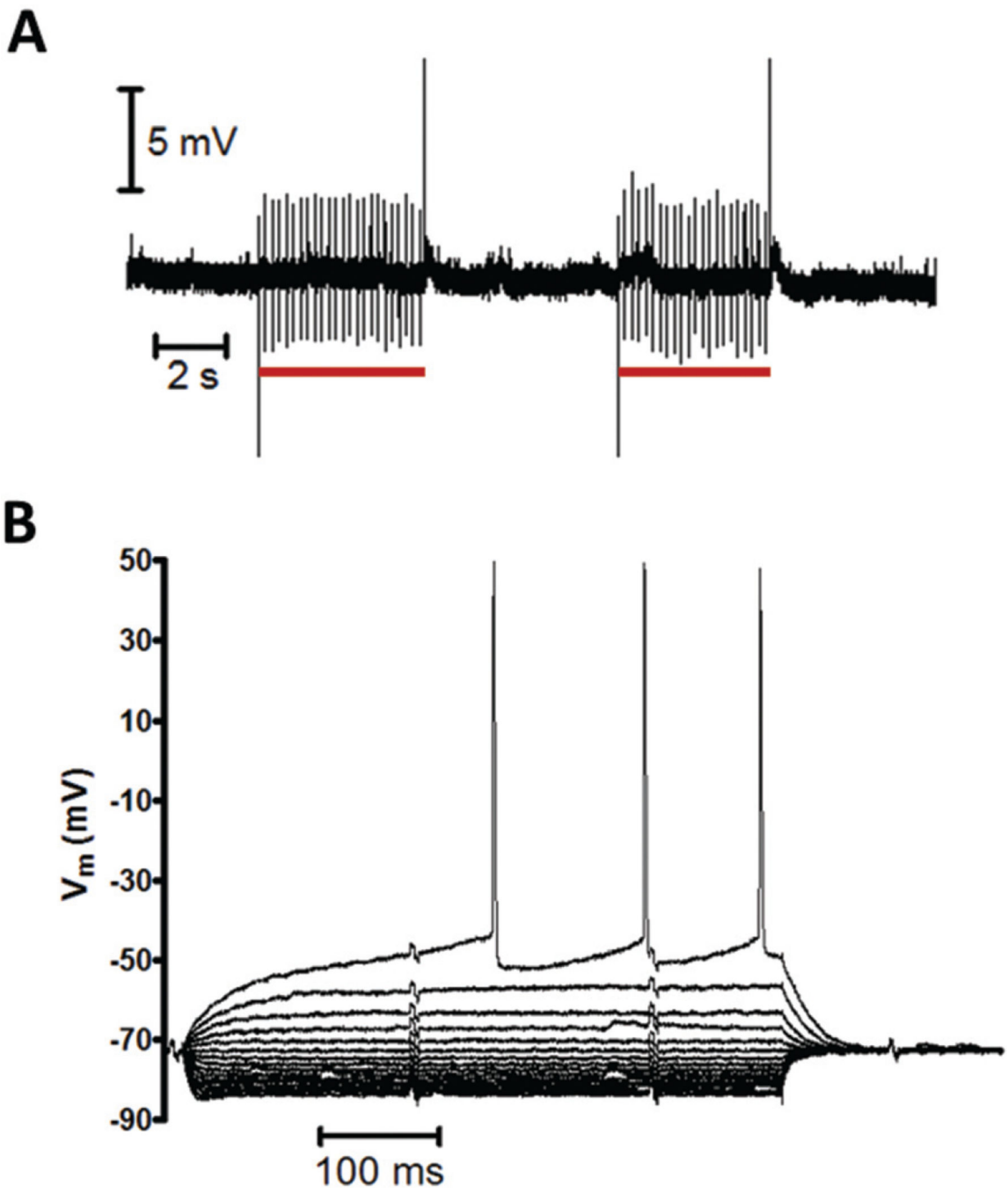

Fig. 5.

Effect of FSCV on neighboring cells. (A) Resting MSN membrane potential during application of FSCV waveform. A current clamp recording of the spontaneous activity of an MSN was obtained in the presence of a carbon fiber performing FSCV. The electrode was positioned adjacent to the cell and the waveform was alternated on (red bars) and off. (B) MSN response to intracellular current injections in the presence of a carbon fiber performing FSCV. Current injections began at −200 pA and increased stepwise by 20 pA until firing was observed. Note that the voltage scale in B is much less than in A.

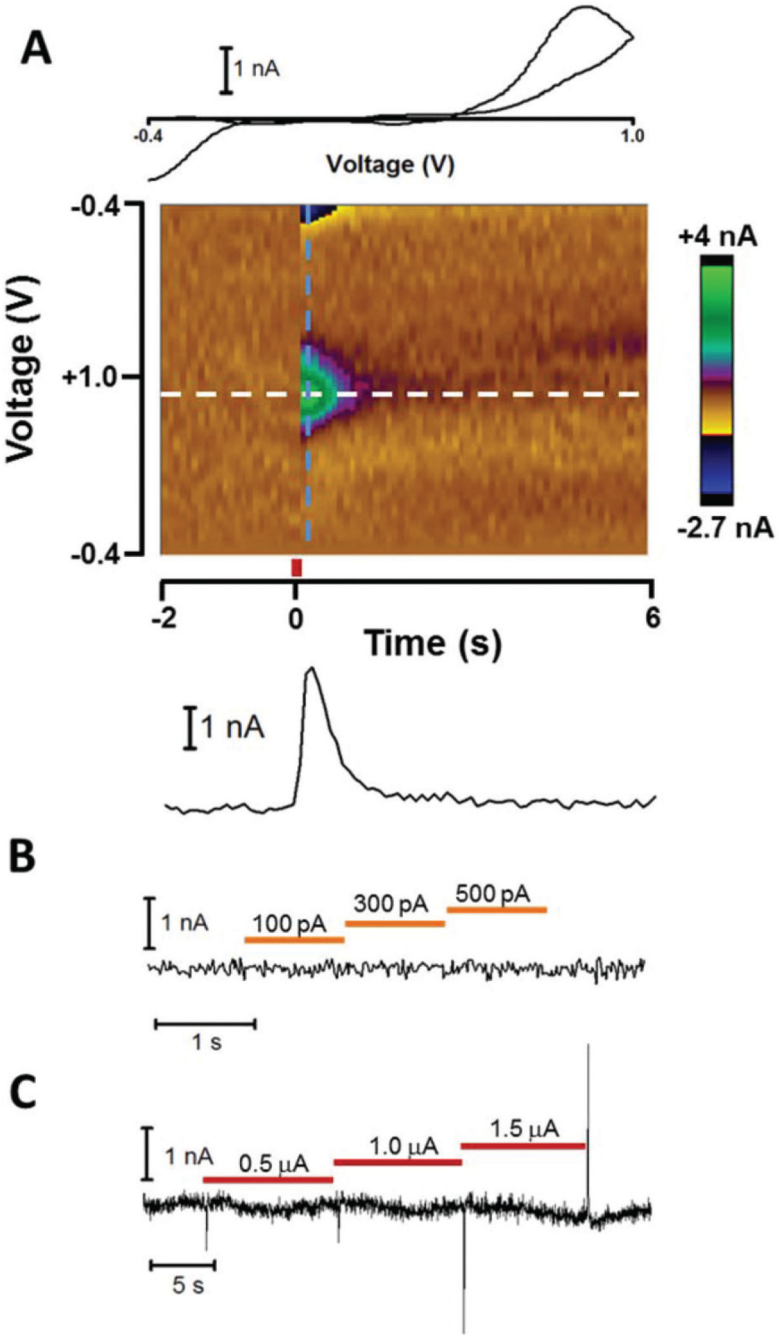

Fig. 6.

Effect of iontophoretic current on neighboring cells. An MSN was depolarized by an intracellular current injection (orange bar), and began firing at a constant frequency. An iontophoresis barrel positioned near the cell delivered the iontophoretic current (red bars).

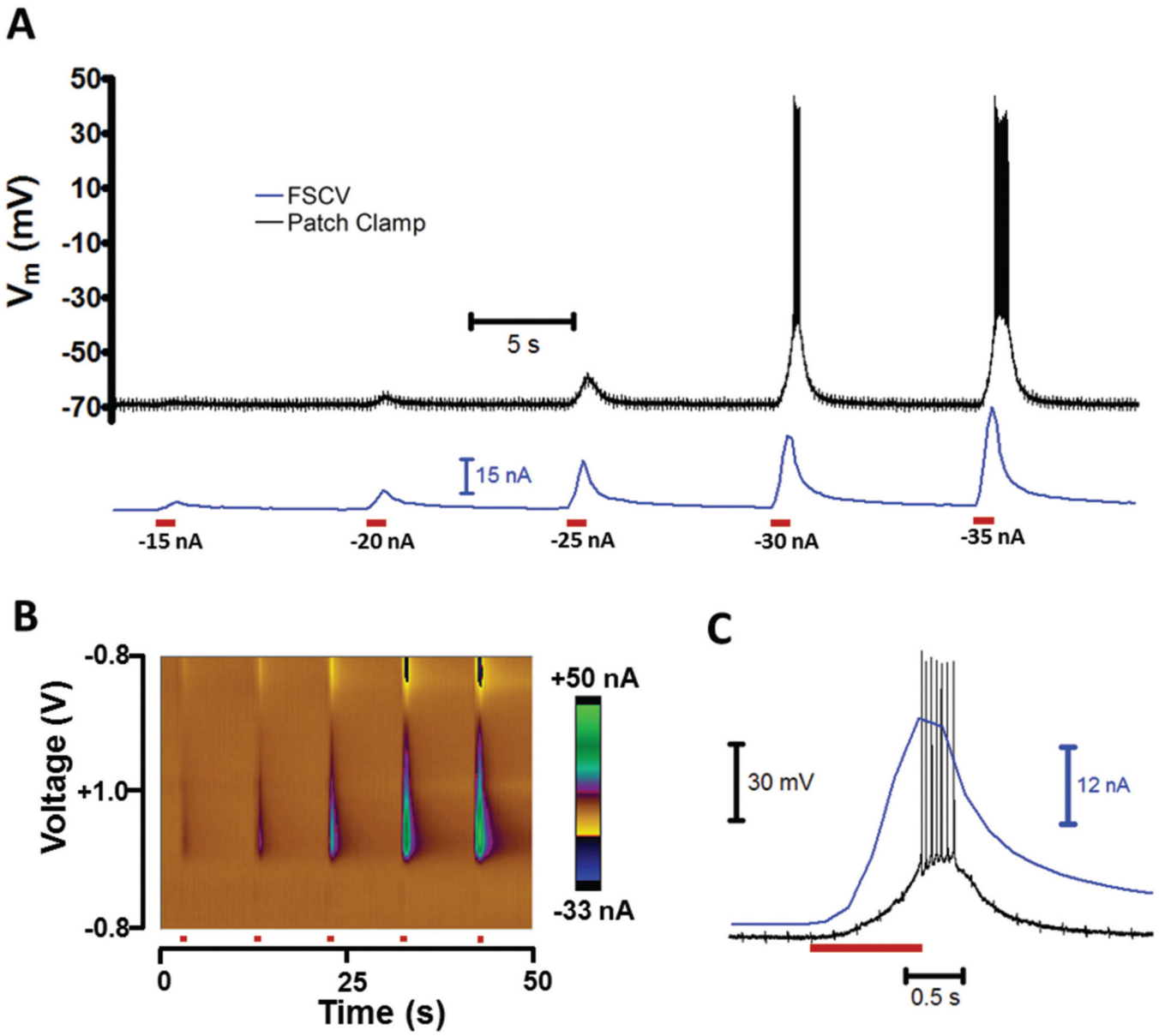

Fig. 7.

Concurrent FSCV and patch recordings during iontophoretic drug administration. (A) Physiological and chemical changes during iontophoretic ejections of glutamate and an electroactive marker. A multibarreled iontophoresis probe positioned ~10 μm from an MSN was used to perform 1 s ejections (red bars) of glutamate, an excitatory neurotransmitter, and DOPAC, the marker. A carbon-fiber electrode on the probe was used to perform FSCV, which detected the ejection of the marker (blue). The cell membrane potential (black) was recorded in a whole-cell current clamp. (B) Color plot of the FSCV current for ejections in A. (C) Time-course of −30 nA ejection in A.

Table 1

Description and values for Fig. 2 circuit components

Symbol	Description	Value
R_s	Extracellular solution resistance	~100 Ω
R_a	Pipette/membrane access resistance	10–35 MΩ
R_m	Cell membrane resistance	30–300 MΩ
R_i	Iontophoresis barrel resistance	0.1–1 GΩ
C_m	Cell membrane capacitance	50–200 pF
R_e	FSCV electrode resistance	~1 MΩ